Acta Cryst. (1998). D**54**, 848–853

A Description of Imperfections in Protein Crystals

COLIN NAVE

CCLRC Daresbury Laboratory, Daresbury, Warrington WA4 4AD, England. E-mail: c.nave@dl.ac.uk

(*Received 11 April 1997; accepted 30 January 1998*)

Abstract

An analysis is given of the contribution of various crystal imperfections to the rocking widths of reflections and the divergence of the diffracted beams. The crystal imperfections are the angular spread of the mosaic blocks in the crystal, the size of the mosaic blocks and the variation in cell dimensions between blocks. The analysis has implications for improving crystal perfection, defining data-collection requirements and for data-processing procedures. Measurements on crystals of tetragonal lysozyme at room temperature and 100 K were made in order to illustrate how parameters describing the crystal imperfections can be obtained. At 100 K, the dominant imperfection appeared to be a variation in unit-cell dimensions in the crystal.

1. Introduction

There has been increasing interest over the past few years in measuring the degree of perfection of protein crystals, normally by determining the rocking widths of individual reflections when illuminated with a highly parallel monochromatic X-ray beam. Such measurements can be used to define the requirements for data-collection facilities as well as to assist in monitoring improvements in crystallization techniques. The rocking widths are often directly assigned to the mosaic spread in the crystal, commonly understood as the angular spread of mosaic blocks in the crystal.

Previous studies of the perfection of protein crystals have concentrated on highly perfect crystals grown on earth and in space using diffractometer-based, Laue or monochromatic topography techniques or combinations of these (Colapietro *et al.*, 1992; Fourme *et al.*, 1995; Snell *et al.*, 1995; Stojanoff *et al.*, 1997). This paper describes crystals with a much lower degree of perfection, corresponding to the protein crystals used in the vast majority of protein-structure determination projects. Freezing of protein crystals is increasingly being used to minimize radiation damage. The rocking width normally increases on freezing to values of 0.2° or more (Mitchell & Garman, 1994), although it is likely that lower values can be obtained. Changes in cell dimensions often occur on freezing. In some cases (*e.g.* Skrzypzak-Jankun *et al.*, 1996) more than one crystal form can exist within the same sample on freezing.

With a large angular spread of mosaic blocks, the spots should be spread into sharp arcs on the diffraction pattern (a powder pattern being the extreme case of this). This effect is often absent despite quite high apparent values of the mosaic spread. Little attention has been given to measuring the angular widths of the diffracted beams from protein crystals. Such measurements can provide extra information about the perfection of the crystals and can also be used in defining data-collection requirements. In this paper, a theoretical analysis is made of the contribution of three types of crystal imperfection to the rocking widths and diffracted-beam divergence. This analysis should have general applicability. In order to illustrate how the various parameters could be determined, measurements on lysozyme crystals at room temperature and 100 K are described. In this case, the increased rocking width at 100 K is better described by a variation in cell dimensions throughout the crystal, rather than an increased angular spread of mosaic blocks.

The issue of crystal perfection is not confined to data collection using highly collimated synchrotron-radiation

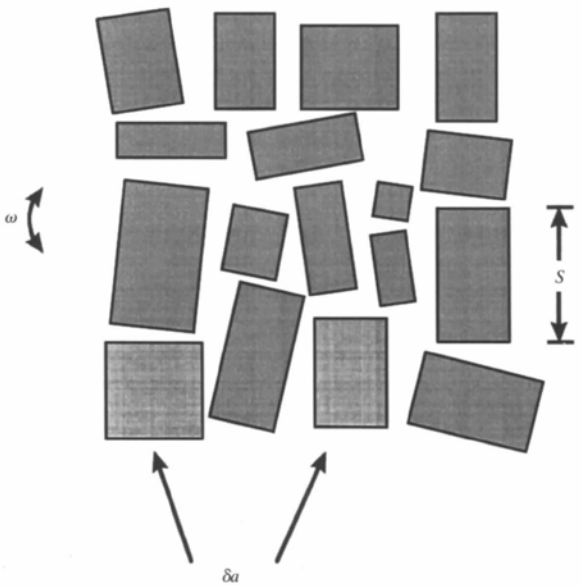

Fig. 1. A mosaic-block model of a crystal showing a spread in the orientation ω of the mosaic blocks, a spread in the size s of the blocks and a variation δa in the cell dimensions between different blocks.

sources. Very well collimated beams can also be obtained from X-ray tubes. The principles of obtaining these beams are described by Arndt (1990).

2. Modelling the imperfections

The purpose of this paper is to describe the imperfections which could occur in common protein crystals. Effects owing to extinction can be safely ignored in these cases, because the structure factors are generally very low and the extinction depth is much larger than the size of the crystal or mosaic block. A discussion of the effects of extinction can be found in Fourme *et al.* (1995).

A simple description of an imperfect crystal is given by a mosaic-block model (Fig. 1). This model is itself also imperfect. Real crystals will have disordered regions. They are likely to have complex dislocation phenomena which might require topographic techniques for analysis (Fourme *et al.*, 1995; Stojanoff *et al.*, 1997). However, the mosaic-block model can be used to introduce three realistic parameters describing the crystal perfection. These parameters are the size s of the mosaic blocks, the angular spread ω of the blocks and the variation in cell dimensions δa (and therefore reciprocal-cell dimensions $\delta a/a^2$) between blocks. These parameters can affect both the angular rocking width of the crystalline reflections and the divergence of the diffracted beams. To simplify the description in this paper, it is assumed that all the blocks are the same size. The values of ω and $\delta a/a$ are assumed to be single numbers which represent the entire range of angles or cell dimensions present in the specimen. The result of these simplifying assumptions is that single numbers are derived for the resultant effects on the diffraction pattern. However, the expressions can be extended to cope with any spread of mosaic-block sizes, angles or cell dimensions within the specimen including, for example, a spread of unit-cell sizes within a mosaic block.

The effects of these specimen imperfections can be derived by considering the broadening of reciprocal-lattice points and the consequences when they pass through the Ewald sphere (Fig. 2). The expressions given cover the case where the reciprocal-lattice point passes normally through the sphere of reflection, which is a reasonable approximation away from the rotation axis in protein-diffraction experiments, but can also be extended to the more general case. The various approximations used here are partly a result of the methods used to characterize the specimen imperfections. Proper evaluation of the parameters requires a complete mapping of the three-dimensional specimen transform in reciprocal space. Useful estimates can be obtained from still images and oscillation images of the diffraction patterns recorded on an area detector.

The three parameters contribute to the observed rocking width in the following manner. In the absence of other effects, the observed rocking width can be equated to the angular spread ω of the mosaic blocks. The effect of mosaic-block size is dependent on the spacing of the Bragg planes d [$= \lambda/(2\sin\theta)$] or its reciprocal d^* ($= 1/d$), the expression for the rocking width being d/s. For the simple case considered here, the effect of the variation in cell dimensions is independent of d and the contribution to the rocking width is $\delta a/a$.

The divergence of the diffracted beam also depends on all three parameters. The angular spread of the mosaic blocks creates spherical caps instead of points in

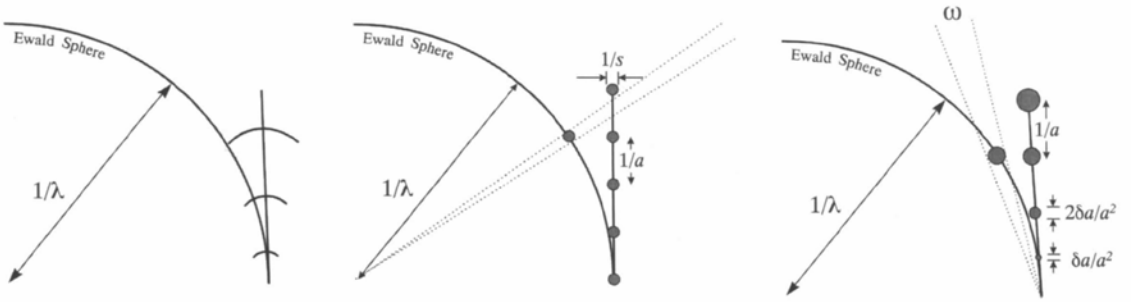

Fig. 2. The effects in reciprocal space of the crystal imperfections shown in Fig. 1. (*a*) The angular spread ω of mosaic blocks leads to spherical caps in reciprocal space. These are represented by arcs in the two-dimensional representation shown here. When the spherical caps pass through the Ewald sphere they are projected onto the detector plane as arcs, in a plane perpendicular to that shown, with an angular spread of ω when measured from the centre of the detector. (*b*) The limited size s of the mosaic blocks leads to a broadening of the reciprocal-lattice points into a distribution which is approximated, for simplicity, by $1/s$ (if a sine function is assumed, corresponding to diffraction from a slit of width s, the distance between the zeros in the transform is actually $2/s$). This distribution subtends an angle of d/s at the origin of reciprocal space, therefore contributing to the rocking width by the same amount. The distribution subtends an angle of λ/s at the origin of the Ewald sphere. This equates to the divergence of the diffracted beam. A reciprocal-lattice point is shown on the sphere of reflection in order to illustrate this. (*c*) The variation in unit-cell dimensions δa leads to an increase in size of the reciprocal-lattice points by an amount $n\delta a/a^2$ which increases with resolution. This distribution subtends an angle of $(n\delta a/a^2)/d^*$ at the origin of reciprocal space. As $d^* = n/a$, this equates to $\delta a/a$ giving this contribution to the rocking width. A reciprocal-lattice point is shown on the sphere of reflection in order to demonstrate this. The distribution subtends an angle of $(\lambda/d)(\delta a/a)$ to the origin of the Ewald sphere. This equates to the divergence of the diffracted beam.

Table 1. *Expressions for the effect of crystal imperfections on reflection rocking width and diffracted-beam divergence*

	Rocking width	Diffracted-beam divergence
Angular spread of blocks ω	ω	arcs of width ω
Mosaic-block size s	d/s	λ/s
Variation in cell dimension $\delta a/a$	$\delta a/a$	$(\lambda/d)(\delta a/a)$

reciprocal space. As they pass through the sphere of reflection, these caps will project on to a flat detector (normal to the beam) to give arcs on the detector of angular width ω. For an ω value of 0.2° the arc will be approximately 0.3 mm long at a distance of 100 mm from the centre of the detector. With commonly used beam sizes and detector resolutions this would only just be observable. The finite size s of the mosaic blocks will lead to broadening of the diffracted beam over an angle of λ/s. This will cause the same increase in the size of a diffraction spot at any resolution. The variation in reciprocal-cell dimensions will give a broadening of $(\lambda/d)(\delta a/a)$. The size of the diffraction spots will therefore increase with distance from the centre of the detector due to the $1/d$ component of the expression.

These effects on rocking width and beam divergence are summarized in Table 1 and further information is given in the caption to Fig. 2. If all three types of imperfection are present, their effects are combined. In general, this would require a convolution of the various distributions to obtain the overall profile of each spot in reciprocal space.

3. Estimating parameters for three types of imperfection

From measurements of rocking width and diffracted-beam divergence at different plane spacings it should be possible to determine values for the three parameters with some redundancy.

For the rocking width, it should be noted that the effect of the angular spread of mosaic blocks and the effect of a variation in cell dimensions will be similar. Both lead to an increase in the size of the average reciprocal-lattice point with resolution (Fig. 2). However, the arcs on the detector created by an angular mosaic spread can be distinguished by inspection from the distribution obtained by a variation in cell dimensions. The latter effect causes the spots to increase in size radially as well as azimuthally.

The measurements on tetragonal crystals of lysozyme at 100 K described below demonstrate how these parameters can be estimated for the type of frozen crystal commonly used for data collection. A highly perfect tetragonal crystal of lysozyme at room temperature was used as a standard, although it was not expected that the experimental setup would provide information on the parameters in this crystal. The preparation of the crystals and freezing techniques were as described in Gonzalez & Nave (1994). The primary aim was to illustrate how the various parameters could be obtained by observing significant effects for the divergence of the

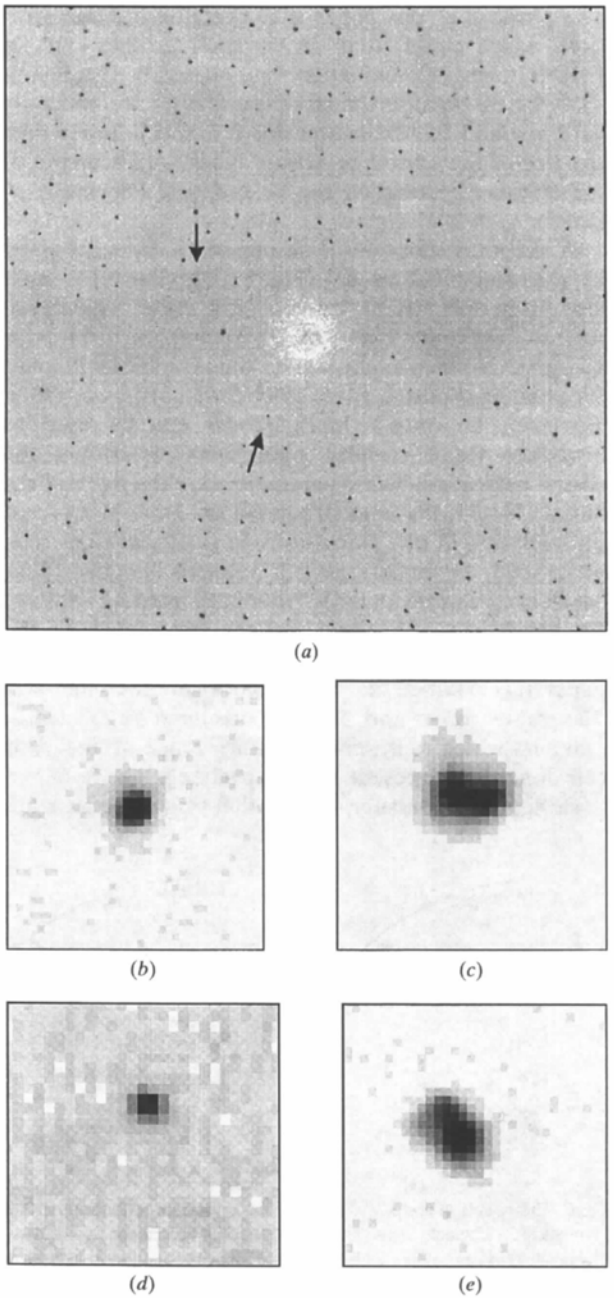

Fig. 3. A measurement of the broadening of the diffracted beam for a tetragonal lysozyme crystal at 100 K. The pixel size is 0.15 mm, the collimator size is 0.2 mm and the beam divergence is 0.3 mrad. (*a*) A diffraction pattern taken at a crystal-to-detector distance of 250 mm. (*b*) and (*d*) Close-ups of the two marked diffraction spots taken at this distance. (*c*) and (*e*) Close-ups of the same diffraction spots taken at a crystal-to-detector distance of 1000 mm.

diffracted beam from a crystal with high mosaicity. Cryoprotectants were therefore not added, although they are often used to obtain a small mosaic spread for the frozen crystal (Mitchell & Garman, 1994).

Station 7.2 on the SRS at Daresbury with wavelength 1.488 Å was used. Slits were used to reduce the horizontal beam divergence to 0.3 mrad, which is comparable with the vertical beam divergence. A 0.2 mm diameter collimator was used. The divergence of the incident beam was checked by recording diffraction spots on X-ray film placed at a distance of 0.6 m from the crystal at room temperature. These diffraction spots were under 0.4 mm in size. This is consistent with a 0.2 mm diameter collimator and a 0.3 mrad divergent beam at 0.6 m from the collimator. The divergence of the diffracted beam was estimated by recording diffraction spots on an image-plate detector (MAR Research) placed at distances between 240 and 1000 mm from the crystal. Oscillation ranges between 2 and 5° were used. For the fully recorded reflections, no significant difference in the diffracted-beam divergence was observed for the different oscillation ranges. Reflection rocking widths were estimated by recording still images and using the *ROTGEN* package (Campbell, 1996) to simulate the observed diffraction pattern. The routines in this program are based on those in the *MOSFLM* processing package (Leslie, 1992). These programs produce a good simulation of a diffraction pattern from a highly perfect stationary crystal, where the number of recorded diffraction spots is determined by the incident-beam divergence and an isotropic mosaic spread, equivalent to ω here. The programs do not simulate the complex shape of the reciprocal-lattice points from some of the frozen crystals and there is no allowance for anisotropy in the mosaic spread. The value of the rocking width obtained was the mosaic spread for which nearly all the observed spots were predicted. Due to the anisotropy of the crystal imperfections, some spots were predicted which were not observed. However, a comparison with parameters obtained from observations of the maximum divergence of the diffracted beams was possible.

4. Results

Fig. 3(*a*) shows a diffraction pattern from the frozen lysozyme crystal taken at a crystal-to-detector distance of 250 mm. Enlargements of two diffraction spots are shown in Figs. 3(*b*) and 3(*d*). These spots, corresponding to *d* values of between 10 and 13 Å, are shown again at a detector distance of 1000 mm in Figs. 3(*c*) and 3(*e*). As shown in Fig. 3, the increase in size is between 3 and 8 pixels (0.45–1.2 mm). The increase may be different in different directions through the spots but is similar for all the spots (approximately 15) in this resolution range. Taken over the extra distance of 760 mm, this corresponds to diffracted-beam divergences of between 0.6 and 1.5 mrad. Similar values were obtained using the spot sizes from room-temperature lysozyme as a reference and measuring the increase in spot size for the low-temperature crystal at a detector distance of 1000 mm. Measurements were also made at *d* spacings of 2.7–3.6 Å on the pattern in Fig. 3(*a*). Several hundred spots were present in this resolution range. Divergences found from reflections with *d* spacings $\simeq$3 Å were approximately four times greater than those obtained with *d* spacings $\simeq$12 Å. The reciprocal-lattice points, therefore, increase in size with increasing plane spacing *d*. Within the error range, the results indicate that the reciprocal-lattice points have a small intrinsic size near the origin of reciprocal space and the contribution due to the finite size of the mosaic blocks is, therefore, small.

Table 2. *Measurements made from diffraction patterns of lysozyme test crystals and parameters describing the crystal imperfections derived from them*

The angular spread ω appears to be small for both crystals. The perfection of the crystal at 290 K is likely to be much better than the limiting values shown here.

	290 K	100 K
Diffraction-pattern measurements		
Rocking width (mrad)	<0.3	15
Diffracted-beam divergence, 10–13 Å resolution	<0.3	0.6–1.5
Diffracted-beam divergence, 2.7–3.6 Å resolution	<0.3	2.0–5.0
Crystal-imperfection parameters		
$\delta a/a$ from rocking width	$<3 \times 10^{-4}$	0.015
$\delta a/a$ from beam divergence, 10–13 Å resolution	$<6 \times 10^{-4}$	0.005–0.012
$\delta a/a$ from beam divergence, 2.7–3.6 Å resolution	$<6 \times 10^{-4}$	0.004–0.013
Mosaic-block size *s* (Å)	>5000	>5000

The results are summarized in Table 2. At room temperature the various measurements were dominated by the beam properties, which is not suprising since lysozyme crystals can have a high degree of perfection (Colapietro *et al.*, 1992; Fourme *et al.*, 1995). A significant increase in rocking width (to 50 times the angular spread of the incident beam) occurred for the frozen crystal. For the frozen crystal (and for the crystal at room temperature) there was no evidence of arcs on the detector produced by a significant angular spread of the mosaic blocks. The spots increased in extent in all directions, though not by the same amounts, and there was some evidence of splitting of the spots (Fig. 3).

The measurements were used to derive the model parameters *s* and $\delta a/a$ (Table 2). The room-temperature crystal is likely to have a high degree of perfection and the parameters obtained from this experimental setup are only limiting values. For the crystal at 100 K, the divergence of the diffracted beams increases with the *d* spacing (Table 2) in a way which indicates that it is dominated by the effect of a variation in the unit-cell

dimensions; in the 10–13 Å spacing range the beam divergence is approximately one quarter of that in the 2.7–3.6 Å spacing range. The values of $\delta a/a$ derived for these ranges are similar, which is consistent with the mosaic-block size making an insignificant contribution to the divergence of the diffracted beams.

The variation in cell dimensions derived from the rocking width and beam divergence agree well. However, it should be pointed out that a single number for the rocking width does not adequately represent the real situation in the frozen crystals.

5. Discussion

The increase in diffracted-beam divergence indicated that the main effect on freezing in this case was to cause a variation in cell dimensions throughout the crystal. This was also the main cause of the observed increase in the rocking width of the reflections. It is common to observe a reduction in cell dimensions on freezing, though not necessarily a distribution of cell dimensions. It is possible that a reduction in cell dimensions is partially dependent on the cooling rate which could vary throughout the depth of the crystal. In some cases (*e.g.* Skrzypzak-Jankun *et al.*, 1996) two distinct phases can coexist in the same crystal, causing problems in data processing.

For a perfect crystal with a single mosaic block the value of s will be the same as the crystal dimensions. This case has been considered by Helliwell (1992) and Snell *et al.* (1995) who derived a value of a/s from the rocking width. The rocking width can only be equated to a/s for the first diffraction order; the correct general expression is a/ns (*i.e.* d/s) for the nth order. The difference affects the theoretical limit for minimum rocking width for a crystal of a particular size. Snell *et al.* (1995) used a beam of 10×20 μrad divergence and observed similar rocking widths for their best space-grown crystal. They stated that this was only a factor of two or so larger than the theoretical limit. The expression given here suggests that the rocking width was in fact much greater than the theoretical limit unless the first diffraction order ($n = 1$) was measured.

The term mosaic spread is often used in data-processing packages as a parameter to assist in predicting the contribution of a particular reciprocal-lattice point to a diffraction image. The term mosaic spread implies a particular type of contribution to the rocking width of each reflection. The analysis here indicates that the rocking width can have a more complex form than that defined (*e.g.* Bolotovsky & Coppens, 1997) by a simple angular spread of mosaic blocks. A more complete description would lead to better results from the data-processing packages, particularly for reflections which are partially recorded on each image. However, the most complete method is to measure three-dimensional profiles of the reflections rather than assume any physically based model.

The observation, in this case, that the variation in unit-cell dimensions is the dominant imperfection provides an explanation for the observation that radially sharp diffraction arcs are not always observed in the presence of high apparent mosaic spreads. If this effect proved to be common, it could provide information to assist in developing procedures for minimizing the effects. It is hoped that further measurements of diffracted-beam divergence will be made in order to further document the effects described here. The synchotron radiation beams used here are sufficiently parallel to investigate these effects for crystals at cryo-temperatures. Cryo-crystallographic techniques are increasingly being used for protein-crystallography data collection. Much more highly parallel beams would be required to estimate the different effects in crystals with a high degree of perfection. There might be difficulty in fully separating all the effects if white-beam methods were used. However, it would be interesting to try white-beam reticulography (Lang & Makepeace, 1996) for examining protein crystals with a high degree of perfection.

The results provide a model to describe the perfection of protein crystals. This can be used to provide a description of the breadth of a reflection in position–angle–wavelength space for a crystal. The use of this formulation to define the requirements for X-ray sources, optics and detectors has been described (Nave, 1998).

The synchrotron radiation beamtime for this investigation was funded by EPSRC grant GR/J87763 awarded to T. J. Greenhough, Keele University for the development of station 7.2 at the SRS. The co-editor and referees are thanked for their helpful suggestions to improve the presentation of these results.

References

Arndt, U. W. (1990). *J. Appl. Cryst.* **23**, 161–168.
Bolotovsky, R. & Coppens, P. (1997). *J. Appl. Cryst.* **30**, 65–70.
Campbell, J. W. (1996). *ROTGEN, A Program for Rotation Images Simulation and Analysis* in *CCP4 Newsletter on Protein Crystallography*, No. 32. Warrington: Daresbury Laboratory.
Colapietro, M., Cappuccio, G., Marciante, C., Pifferi, C., Spagna, R. & Helliwell, J. R. (1992). *J. Appl. Cryst.* **25**, 192–194.
Fourme, R., Ducruix, A., Riès-Kautt, M. & Capelle, B. (1995). *J. Synchrotron Rad.* **2**, 136–142.
Gonzalez, A. & Nave, C. (1994). *Acta Cryst.* D**50**, 874–877.
Helliwell, J. R. (1992). *Macromolecular Crystallography with Synchrotron Radiation*, ch. 2, pp. 24–26. Cambridge University Press.
Lang, A. R. & Makepeace, A. P. W. (1996). *J. Synchrotron Rad.* **3**, 313–315.

Leslie, A. (1992). *Recent changes to the MOSFLM package for processing film and image plate data* in the *Joint CCP4 and ESF-EACBM Newsletter on Protein Crystallography*, No. 26. Warrington: Daresbury Laboratory.

Mitchell, E. P. & Garman, E. F. (1994). *J. Appl. Cryst.* **27**, 1070–1074.

Nave, C. (1998). *J. Synchrotron Rad.* **5**, 645–647.

Skrzypzak-Jankun, E., Bianchet, M. A., Amzel, L. M. & Funk, M. O. Jr (1996). *Acta Cryst.* D**52**, 959–965.

Snell, E. H., Weisgerber, S., Helliwell, J. R., Weckert, E., Hölzer, K. & Schroer, K. (1995). *Acta Cryst.* D**51**, 1099–1102.

Stojanoff, V., Siddons, D. P., Monaco, L. A., Vekilov, P. & Rosenberger, F. (1997). *Acta Cryst.* D**53**, 588–595.